Cerebral Cortex May 2011;21:1213–1221
doi:10.1093/cercor/bhq206
Advance Access publication October 20, 2010

The Relationship of Gamma Oscillations and Face-Specific ERPs Recorded Subdurally from Occipitotemporal Cortex

Andrew D. Engell and Gregory McCarthy

Human Neuroscience Laboratory, Department of Psychology, Yale University, New Haven, CT 06520-8205, USA

Address correspondence to Gregory McCarthy, Department of Psychology, Yale University, PO Box 208205, New Haven, CT 06520-8205, USA. Email: gregory.mccarthy@yale.edu.

The perception of faces evokes characteristic electrophysiological responses at discrete loci in human fusiform gyrus and adjacent ventral occipitotemporal cortical sites. Prominent among these responses are a surface-negative potential at ~200-ms postonset (face-N200) and face-induced spectral perturbations in the gamma band (face-γERSP). The degree to which these responses represent activity in the same cortical loci and the degree to which they are influenced by the same perceptual and task variables are unknown. We evaluated this anatomical colocalization and functional correlation in 2 experiments in which the electrocorticogram was recorded from subdural electrodes in 51 participants. Experiment 1 investigated the category specificity of the γERSP and its colocalization with the face-N200. Experiment 2 examined differences in face-N200 and face-γERSP to face stimuli that varied in featural complexity. We found that γERSP is a category-specific phenomenon with separate, though overlapping, category sensitivities as the N200. Further, the presence of face-γERSP at an electrode site significantly predicted the presence and amplitude of face-N200 at that site. However, the converse was not true in that face-N200 was evoked by impoverished face stimuli that did not induce face-γERSP. These results demonstrate that these electrophysiological responses reflect separate components of the brain's face processing system.

Keywords: ECoG, ERP, face, gamma, vision

Introduction

Face processing is a highly developed competence of the primate visual system. Psychological models of face processing posit a sequence of component processes beginning with low-level structural encoding and proceeding to higher level processes for facial expression analysis and person identification (Bruce and Young 1986). Electrophysiological and functional neuroimaging studies in humans (e.g., Sergent et al. 1992; Haxby et al. 1994; Allison, Ginter, et al. 1994; Puce et al. 1995; Kanwisher et al. 1997; Allison et al. 1999; McCarthy 2001) and nonhuman primates (e.g., Gross et al. 1972; Bruce et al. 1981; Perrett et al. 1982; Tsao et al. 2003; Pinsk et al. 2005) have identified several discrete nodes of face-specific activity, which suggests that at least some of the component processes identified in psychological studies may be instantiated in a hierarchy of neural processing stages distributed throughout the brain. While the anatomical loci of these processing nodes have become established, their distinguishing functions have become the focus of intense interest.

Electrophysiological recordings in humans from subdural electrodes placed on the fusiform gyrus and nearby locations within ventral occipitotemporal cortex (VOTC) have revealed a face-specific event-related potential (ERP) that appears as a cortical surface-negative potential that peaks at ~200 ms (face-N200) after the onset of a face stimulus (Allison, Ginter, et al. 1994; Allison et al. 1999; McCarthy 2001). The face-N200 is discretely distributed within the VOTC, with most sites across subjects occurring on the fusiform gyrus. At many of these sites, the face-N200 occurs as the most prominent among a triphasic temporal sequence of potentials that includes cortical surface–positive potentials that peak at ~150 ms (P150) and ~290 ms (P290). One of the more surprising results from the initial studies of the VOTC face-N200 was its insensitivity to task manipulations, leading to the conclusion that the face-N200 represents an early and obligatory stage of face processing, such as structural encoding (Allison, Ginter, et al. 1994). Longer latency face-specific ERPs in the ventral anterior temporal lobe were more sensitive to person identity, and thus, it was proposed that more elaborative face processing occurred there (Puce et al. 1999).

The discovery of gamma oscillations (>30 Hz) induced during face perception and recorded from electrodes along the VOTC (Lachaux et al. 2005; Tsuchiya et al. 2008; Fisch et al. 2009; Engell and McCarthy 2010) has motivated a reexamination of the conclusions about the functional characteristics of face processing in the VOTC drawn from these earlier ERP studies. While subdurally recorded ERPs have provided considerable information about localized information processing in the brain, the signal-averaging approach used in ERP recording discards as noise oscillatory potentials that are not precisely phase locked across trials. Nevertheless, these non–phase-locked potentials may provide important information about the sensitivity of a brain region to task manipulations that is not evident in the phase-locked ERPs.

The functional relationship between face-induced gamma event-related spectral perturbations (face-γERSP) and the face-N200 and other face-specific ERPs recorded from the VOTC is as yet largely unknown. Indeed, whether face-N200 and other face-ERPs are spatially colocalized at VOTC sites with face-γERSP is undecided by the current literature. However, even when examined at the same electrode sites, it is unclear whether the face-γERSP and the face-N200 reflect different functions within the face processing system. In a recent study, we demonstrated that the face-γERSP recorded from the VOTC was sensitive to the allocation of attention to faces in a task in which subjects viewed a complex stimulus array consisting of both faces and houses, while the face-N200 at the same electrode sites remained unaffected (Engell and McCarthy 2010). Though this result suggests a functional dissociation between face-γERSP and face-N200, it is possible that the attentional enhancement of the face-γERSP reflects a prolongation of the same processing reflected by face-N200 rather than

a separate aspect of face processing, per se. That is, the dissociation may be quantitative rather than qualitative.

Here we report 2 experiments in which the electrocorticogram (ECoG) was recorded directly from the cortical surface of 51 patients being evaluated for epilepsy surgery (Spencer et al. 1982). Experiment 1 investigated the category specificity of the induced gamma response and its spatial proximity to the face-N200 by showing patients series of exemplars from different visual stimulus categories that included faces, animals, tools, fruits and vegetables, and letter strings. The inclusion of animals was particularly important as the γERSP response to faces has yet to be formally contrasted with nonhuman animals (but see Fisch et al. 2009 for an informal comparison), and there is evidence that the primate brain is sensitive to the categorical distinction between animate and inanimate objects (e.g., Kiani et al. 2007). Our data reveal a large face-specific increase in broadband gamma power (face-γERSP) that is spatially localized to sites that also show a face-specific evoked response. Moreover, we find that at these locations the evoked (i.e., ERP) and induced (i.e., ERSP) responses evince different sensitivities to nonface categories (i.e., between-category differences), particularly animals, suggesting that the functional dissociability of these responses is due to more than simple task-dependent processing.

Experiment 2 further tests this notion by examining differences in face-N200 and face-γERSP to face stimuli that vary dramatically in featural complexity. Consistent with the results of Experiment 1, we find that the response properties of the evoked face-N200 to within-category differences differ dramatically from those of the induced face-γERSP, demonstrating that these electrophysiological responses reflect separate components of the brain's face processing system.

Materials and Methods

EEG Acquisition

Recordings were obtained from 51 patients (median age = 27 years, age range: 7–54 years, 29 female, 22 male) with medically intractable epilepsy who were being evaluated for possible surgery by the Yale Epilepsy Surgery Program (Spencer et al. 1982). In these patients, strips or grids of stainless steel electrodes (2.2-mm surface diameter) were placed subdurally on the cortical surface. The placement of the strips was determined by the clinical needs of each patient, and thus, electrode locations varied across individuals. The studies reported here were among several sensory and cognitive ECoG experiments in which each subject participated, typically 4–8 days following implantation of electrodes. At the time of participation, medication levels to control seizures and postoperative pain varied across patients. The EEG experiments were not conducted immediately before or after seizures nor were any of our sites of interest revealed to be in epileptogenic cortex. The EEG protocol was approved by the IRB of the Yale University School of Medicine. All participants provided informed consent.

Local field potentials were recorded simultaneously from 128 electrode sites and amplified with a common reference (either the mastoid or a small post electrode implanted in the patient's skull) using an SA Instruments EEG amplifier system with a 0.1- to 100-Hz bandpass. From each patient, we simultaneously recorded from 128 electrodes with a concentration of sites on VOTC and lateral occipital, posterior lateral temporal, and parietal cortices. The EEG signal was continuously acquired and digitized with 14-bit resolution using a Microstar 4200 A/D data acquisition board. The digitized signal was sampled at 250 Hz and written to disk using a custom PC-based acquisition system. Signal from the 6 most recent patients was sampled at 500 Hz and then downsampled to 250 Hz prior to analysis. A digital code unique to each experimental condition was recorded in a separate channel at the onset of each stimulus presentation.

Forty-one patients participated in Experiment 1, which consisted of a "screening" task designed to identify face-specific N200 electrode sites. Thirty-seven patients participated in Experiment 2, including 27 who also participated in Experiment 1. Data collection for Experiment 2 occurred over several years, during which time there was a change in the stimuli used for the screening task. As a result, 10 of the patients participated in screening tasks very similar to Experiment 1, but which included different category images.

Stimuli

Stimulus presentation was computer controlled and displayed on a CRT monitor (640 × 480 pixels) positioned on a table over the patient's bed. The viewing distance was adjusted for patient comfort.

Stimuli in Experiment 1 included color images from one of 6 categories: animals, faces, fruits and vegetables, letter strings, scrambled faces, and tools (Fig. 1*b*). Sixty unique exemplar images were included for each category. The scrambled faces were constructed by performing a 2D Fourier transform of each face stimulus, permuting the phase spectrum, performing an inverse transform, and correcting for overall luminance. These phase-scrambled faces thus had the same spatial frequencies as the face stimuli but were unrecognizable as faces.

Stimuli in Experiment 2 included feature-rich "complex" faces, feature-poor "simple" faces, and greeble objects (Gauthier and Tarr 1997). Sixty complex faces (30 male and 30 female) were created using the Poser software package (Smith Micro Software) to be

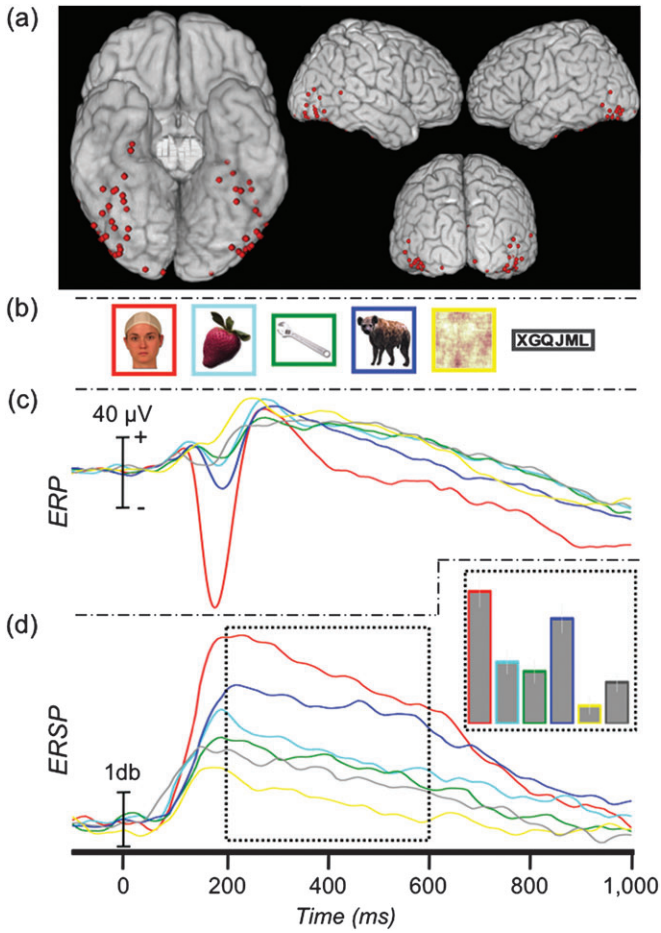

Figure 1. Face-specific ERP and ERSP. (*a*) Location of 58 face-N200 sites displayed on a standard brain. (*b*) Example stimuli presented to patients in Experiment 1. (*c*) The grand-average ERP at the face-N200 sites. (*d*) The average γERSP time course at the face-N200 sites and AUC (inset).

pseudo-realistic with texture, depth, and coloring (Fig. 7*b*). Simple face stimuli were 60 high contrast line drawings of schematic faces that included an oval outline and lines for eyes, nose, and mouth. Sixty greeble objects were included as a nonface control stimulus as they have been characterized as "similar to faces along several dimensions" (Gauthier and Tarr 1997) and because they were colored objects similar to our complex faces in texture and depth.

Procedure

In both experiments, patients were asked to view sequentially presented stimuli that were randomly selected from task relevant categories (6 categories in Experiment 1, 3 categories in Experiment 2, see above). In total, patients viewed 60 unique exemplars from each stimulus category. Each image was displayed for 500 ms with a jittered stimulus-onset asynchrony that varied randomly between 1800 and 2200 ms. To ensure the patient's engagement with the task, a target circle was presented on approximately ~12% of trials to which a speeded button press response was required. Presentation of the stimuli was intermittently paused to give the patients a rest period.

ERP Analysis

ERP analyses were performed using custom MATLAB (The Mathworks, Inc.) functions. Residual line noise (60 Hz) filtering was performed in Matlab using a fifth-order Butterworth filter that was applied in a temporally symmetric manner to avoid introducing phase shifts. Baseline adjusted ERPs were created by signal averaging the EEG signal across trials for each experimental condition and subtracting from each time point the average of a 100-ms prestimulus epoch. A temporally symmetric smoothing kernel with a total length of 5 time points (from –2 to +2 time points) was convolved with the average ERP waveforms prior to amplitude and latency measurements of P150, N200, and P290.

The data from Experiment 1 (or a similar screening task) were used to identify electrodes demonstrating category specificity to faces. Guided by previously published criteria (Allison et al. 1999), face-specific sites were defined as those with a peak negativity occurring between 160- and 240-ms poststimulus onset (N200) that was at least –50 μV in amplitude and at least twice as large to faces than to any other stimulus categories (not including animals, see below). Similar selection criterion (i.e., a category response twice as large as to all other tested categories) has previously been used in both single cell (e.g., Perrett et al. 1982; Baylis et al. 1985; Leonard et al. 1985) and human local field potential (e.g., Puce et al. 1997, 1999; Allison et al. 1999; McCarthy et al. 1999) investigations of face specificity. A computer algorithm was used to identify potential face-specific sites for visual inspection by the authors to screen for artifacts.

Animals were not included in the test for face specificity because it has previously been shown that frontal views of faces of cats and dogs evoke a response ~75% the magnitude of human faces (McCarthy et al. 1999), and many of our animal stimuli included the animal's face. In order to test the effect of face visibility in the animal pictures, we sorted the animal pictures into new categories of "animal-toward," those in which an animal's face was prominently displayed, and "animal-away," those in which the face was obscured or not conspicuous (see Fig. 4*a*). Faces were included so that the relative response of animal-toward could be evaluated against the evoked and induced face-specific response. Tools were included to serve as a nonbiological control stimulus. The remaining categories were omitted to avoid redundancy and to simplify visualization of the results.

The ERP amplitudes and latencies at these face-specific locations were analyzed with separate one-way analyses of variance (ANOVAs). Sphericity violations were addressed by adjusting the degrees of freedom using the Greehouse–Geisser method (only the unadjusted degrees of freedom are reported in the Results section). Planned comparisons using paired *t*-tests further explicated significant main effects. Bonferroni corrections of the family-wise error rate ($P_{FW} < 0.05$) for exploratory post hoc contrasts were applied where appropriate and, unless specified, all *P* values reported for post hoc contrasts are "corrected" *P* values.

We have previously reported that the face-N200 is highly spatially localized (see Fig. 2). That is, the evoked potential recorded at a given electrode is often not evident at adjacent electrode sites. To compare spatial specificity for face-N200 and face-γERSPs, we created ERPs and γERSPs from non–face-specific recording sites immediately adjacent to face-N200s (face-N200 neighbor sites). The only criteria for these sites were that they were immediately adjacent (≤10 mm) to an electrode showing a face-specific N200 and did not themselves meet the criteria for face specificity. Importantly then, this did not preclude the inclusion of "face-sensitive sites," sites at which the N200 to faces was larger than to all other categories but did not reach our minimum criteria of twice as large as other categories or a minimum of –50 μV.

ERSP Analysis

Prior to ERSP analysis, we removed the mean (unsmoothed) signal-averaged ERP from the raw EEG signal for each trial. This ensured that any significant spectral differences between categories did not merely reflect the frequency composition of the phase-locked ERP. As a result of this approach, the frequency-domain analysis reported here is insensitive to spectral changes that undergo phase resetting (i.e., phase-locked "evoked" EEG responses). However, these spectra are captured in the time-domain analysis (i.e., ERP), resulting in a full characterization of the data. Moreover, the evoked face-N200 is a low-frequency response that is not reflected in the gamma band (Engell and McCarthy 2010).

Event-related spectral perturbations (ERSP) were computed using EEGLAB v7.1 (Delorme and Makeig 2004) and MATLAB v7.9 (The Mathworks, Inc.). Time-frequency power spectra were estimated using Morelet wavelet analysis based on 3 cycles at the lowest frequency (11.6 Hz) increasing to 16 cycles at the highest frequency (125 Hz). Change in power induced by each category (i.e., ERSP) was estimated by calculating the ratio of log power (db) between the poststimulus and prestimulus epochs. ERSPs within the gamma band (30–100 Hz) (γERSP) were averaged at each time point to create a "gamma power-wave" over time. This frequency range for gamma was selected on the basis of the prior literature. Reports in the animal (Singer and Gray 1995; Tallon-Baudry and Bertrand 1999) and human (Lachaux et al. 2005; Tsuchiya et al. 2008; Fisch et al. 2009; Engell and McCarthy 2010) literatures have defined 30 Hz as the lower bound of the gamma band. Human intracranial studies have reported an upper bound for gamma between 70 and 200 Hz (Lachaux et al. 2005; Tsuchiya et al. 2008; Fisch et al. 2009; Engell and McCarthy 2010). The amplifiers used in our studies imposed a 100-Hz (–3 db) upper limit on the ECoG signal, and so we restricted the upper range of the gamma band to 100 Hz. A one-way ANOVA was used to analyze the area under the curve (AUC) estimates between 200- and 600-ms poststimulus at face-N200 sites. The interval between 200 and 600 ms was selected after inspection of the grand-average time-frequency plots from each condition in Experiment 1 (see Supplementary Figure 1). Across conditions, this time window captured the largest changes in gamma power. Corrections for sphericity violations and multiple comparisons were the same as those used for the ERP analysis.

In order to explore properties of the evoked response at face-γERSP electrode sites that did not also have a face-specific N200, we identified all electrodes with a minimum AUC of 100 db^2 between 200- and 600-ms poststimulus that was also 50% larger than the AUC induced by any other condition other than animals.

Electrode Localization

To facilitate visualization of the electrode locations across participants, the approximate location of each face-N200 and face-γERSP recording site was represented on the ventral surface of a standard brain. A high-resolution anatomical scan (1 × 1 × 1.5 mm) was acquired for each patient prior to implantation. Postimplant CT scans in which the electrodes were easily detected and localized in 3D were then coregistered to the anatomical magnetic resonance data. Each patient's brain was warped to Montreal Neurological Institute space using the Bioimage Suite software package (http://www.bioimagesuite.org) to facilitate visualization of recording sites from all patients on a standard brain. In cases in which the inherent imprecision of spatial normalization resulted in an electrode appearing to hover immediately above the brain surface, the electrode position was projected to the cortical surface. This approach allowed for a convenient graphical representation of the overall distribution of electrodes on the brain's

surface. However, as the exact gyral and sulcal boundaries of the brain varied among our subjects, this summary view does not precisely reflect the exact position of any individual electrode.

Results

Experiment 1—Face Specificity: ERP

We recorded from 5248 sites from 41 patients in Experiment 1. Fifty-eight (1.1%) face-specific sites (32 right hemisphere and 26 left hemisphere) were identified from 30 patients, primarily along the VOTC and adjacent lateral regions including inferior and middle temporal and inferior occipital and middle occipital cortices (Fig. 1*a*). These 30 patients each had between 1 and 8 (median = 2) face-specific sites. At these sites, faces evoked a sharp negative potential (mean of −112 μV, Table 1) that peaked a mean of 189 ms (face-N200) after onset of the face. Figure 1*c* shows the grand average of these responses. Note that the peak amplitude of the grand average is somewhat smaller than the mean of each subject's N200 amplitude due to subject-to-subject latency variation. An independent samples *t*-test demonstrated that neither the amplitude (μV) nor latency (ms) of this response varied as a function of hemisphere ($t_{(56)}$ = 0.46, P = 0.648 and $t_{(56)}$ = 0.14, P = 0.887, respectively), so all subsequent analyses were collapsed across hemispheres.

Table 1
Experiment 1: ERP and ERSP (AUC between 200 and 600 ms) response at face-N200 sites

Condition	ERP				ERSP	
	Amplitude (μV)		Latency (ms)		Gamma AUC (db^2)	
	Mean	SD	Mean	SD	Mean	SD
Faces	−111.9	58.1	189.0	18.1	109.6	103.1
Fruits	−5.3	53.7	189.4	23.5	43.9	78.6
Tools	−0.9	24.9	187.7	27.1	36.6	82.9
Animals	−12.9	30.2	192.6	23.9	79.1	86.4
Face toward	−27.1	36.2	197.4	24.8	81.9	95.1
Face away	−3.8	31.0	191.7	24.5	67.7	86.6
Scrambled faces	3.3	28.7	185.3	27.3	5.1	47.7
Letter strings	−6.1	41.7	183.0	27.9	34.6	74.8

Note: SD, standard deviation.

Stimulus category significantly affected amplitude ($F_{5,285}$ = 111.38, P < 0.001) but not latency ($F_{5,285}$ = 1.58, P = 0.165). Planned comparisons confirmed that the peak amplitude to faces was significantly greater than to fruits ($t_{(57)}$ = 14.01, P < 0.001), tools ($t_{(57)}$ = 13.62, P < 0.001), animals ($t_{(57)}$ = 12.01, P < 0.001), scrambled faces ($t_{(57)}$ = 14.13, P < 0.001), and letter strings ($t_{(57)}$ = 13.09, P < 0.001). It is important to note that these amplitude results were expected given our selection criteria. However, statistical analyses were nonetheless performed to compare peak latencies and to facilitate comparisons with subsequent analysis. Post hoc tests also showed that, at these sites, the response to animals was greater than to fruits, tools, and scrambled faces (all P values < 0.05). The animal ERP was also greater than letter strings, though this contrast was not significant after correcting for multiple comparisons (P = 0.02, "uncorrected").

At face-N200, neighbor sites stimulus category significantly affected amplitude ($F_{5,285}$ = 5.08, P < 0.001) but not latency ($F_{5,285}$ = 1.67, P = 0.326) (Fig. 3*b*). Planned comparisons showed that the peak amplitude to faces was significantly greater than to fruits ($t_{(57)}$ = 3.79, P < 0.001), tools ($t_{(57)}$ = 5.02, P < 0.001), animals ($t_{(57)}$ = 3.22, P = 0.002), and letter strings ($t_{(57)}$ = 2.77, P = 0.008). The response to faces was larger than to scrambled faces, but this difference was only marginally significant ($t_{(57)}$ = 1.97, P = 0.054). Post hoc tests did not reveal any other significant pairwise differences after correcting for multiple comparisons.

Experiment 1—Face Specificity: γERSP

There was a significant effect of category on gamma amplitude ($F_{5,285}$ = 44.28, P < 0.001) (Fig. 1*d* and Supplementary Figure 1). Planned comparisons showed that the γERSP to faces was significantly larger than to fruits ($t_{(57)}$ = 5.78, P < 0.001), tools ($t_{(57)}$ = 7.23, P < 0.001), animals ($t_{(57)}$ = 2.97, P = 0.004), scrambled faces ($t_{(57)}$ = 9.30, P < 0.001), and letter strings ($t_{(57)}$ = 7.70, P < 0.001). Post hoc contrasts of all remaining pairwise differences revealed that the γERSP to animals was significantly larger than to all nonface categories (all P values < 0.05) and that the γERSP to scrambled faces was significantly smaller than all other categories (all P values < 0.05).

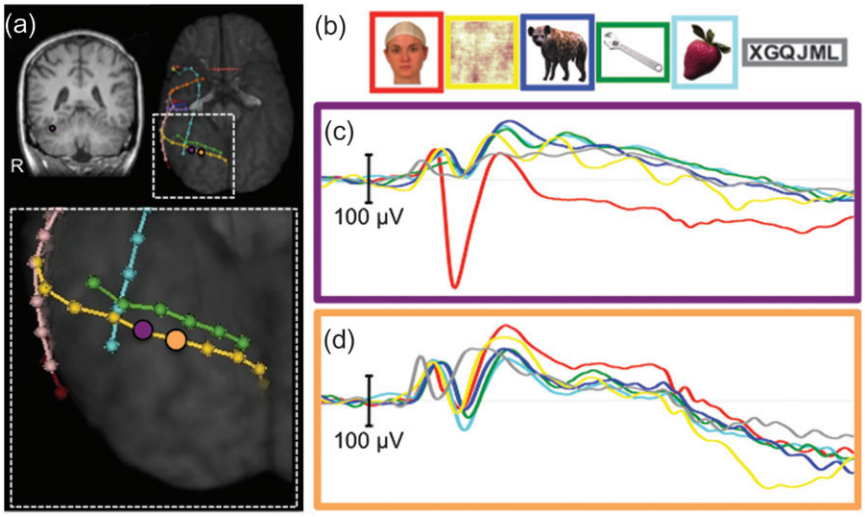

Figure 2. Spatial extent of N200. (*a*) Electrode strips localized on the ventral surface of a representative patient. A face-specific N200 was found at the recording site indicated by a purple ellipse. The orange ellipse indicates an adjacent non–face-specific location. (*b*) Example stimuli from each of the 6 stimulus categories. (*c*) The average ERPs recorded from this patient from the purple electrode site. (*d*) The average ERPs recorded from this patient from the orange electrode site.

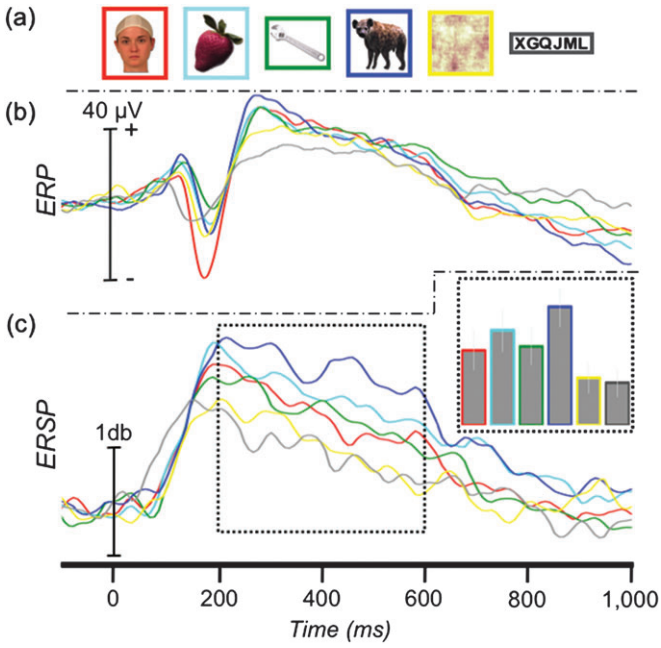

Figure 3. ERP and ERSP response at N200-adjacent recording sites. (*a*) Example stimuli presented to patients in Experiment 1. (*b*) The grand-average ERP at locations immediately adjacent (~10 mm) to the 58 face-N200 sites. (*c*) The average γERSP time course and AUC (inset) at locations immediately adjacent to the 58 face-N200 sites.

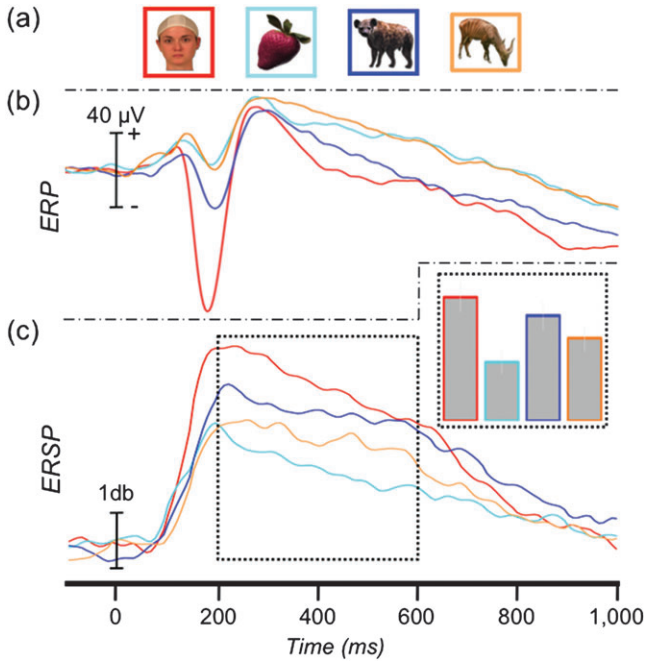

Figure 4. ERP and ERSP to animals. (*a*) Example stimuli presented to patients in Experiment 1. Animal stimuli have been separated into those with and without a highly visible face. (*b*) The grand-average ERP at the 58 face-N200 sites. (*c*) The average γERSP time course and AUC (inset) at the 58 face-N200 sites.

At face-N200 neighbor sites, there was a significant effect of category on gamma amplitude ($F_{5,285}$ = 7.87, P < 0.001) (Fig. 3*c*). Planned comparisons showed that the gamma response to faces was significantly smaller than to animals ($t_{(57)}$ = −3.21, P = 0.002). No other pairwise comparisons with faces were significant (all P values > 0.05). Post hoc pairwise contrasts of animals to all remaining nonface categories showed that the animal-induced γERSP was larger than tools, scrambled faces, letter strings (all P values < 0.05), and fruits (P = 0.033, uncorrected).

Experiment 1—Effect of Animal Faces: ERP

Separate one-way ANOVAs (4 levels: faces, fruits, animal-away, and animal-toward) showed a significant main effect of category on peak amplitude ($F_{3,171}$ = 124.50, P < 0.001) but not on peak latency ($F_{3,171}$ = 1.42, P = 0.239) of the N200 (Fig. 4*b*). Pairwise contrasts showed that the peak amplitude to faces was larger than to all other conditions (all P values < 0.05). We also found that the peak response to animal-toward was significantly larger than to both animal-away ($t_{(56)}$ = 5.63, P < 0.05) and fruits ($t_{(56)}$ = 7.22, P < 0.05), whereas there was no difference between animal-away and fruits ($t_{(56)}$ = 1.07, P = 0.291).

Experiment 1—Effect of Animal Faces: γERSP

As with the ERP analysis, we tested the effect of facial visibility in the animal pictures on the gamma response. A one-way ANOVA (4 levels: faces, fruits, animal-away, and animal-toward) showed a significant main effect of category ($F_{3,171}$ = 19.69, P < 0.001) (Fig. 4*c*). The γERSP to faces was larger than to fruits ($t_{(57)}$ = 5.72, P < 0.05), animals-away ($t_{(57)}$ = 3.88, P < 0.05), and animals-toward, though this difference did not survive correction for multiple comparisons ($t_{(57)}$ = 1.97, P = 0.054, uncorrected). The γERSP to animals-toward was significantly larger than both fruits ($t_{(57)}$ = 5.36, P < 0.05) and animal-away ($t_{(57)}$ = 3.07, P < 0.05). Animals-away was significantly larger than fruits ($t_{(57)}$ = 3.44, P < 0.05).

Experiment 1—ERP and γERSP Relationship

We investigated the relationship between the evoked ERP and induced γERSP at face-N200 sites. Correlation analysis of the face-N200 magnitude, defined as the peak-to-peak difference between the N200 and P150 (peak positivity in the 75 ms preceding the N200), and the γERSP magnitude, defined as the AUC between 200- and 600-ms poststimulus, revealed a significant positive linear relationship, $r_{(56)}$ = 0.50, P < 0.001 (Fig. 5*a*). However, inspection of the response at these sites reveals that not all face-N200 sites were associated with increased gamma oscillations (see data points in Fig. 5 with near zero N200 amplitudes depicted along the *y*-axis).

We next identified sites that showed a face-γERSP (see Materials and Methods). Of the 39 face-γERSP sites, 17 had previously been identified as face-N200 sites whereas the remaining 22 (0.4% of all recording sites) did not have a concomitant face-specific N200, as defined by our conservative selection criteria (Fig. 6*a*). The cortical distribution of these 3 types of functionally defined sites (face-N200 and face-γERSP, face-N200 only, and face-γERSP only) is displayed in Supplementary Figure 2. The onset and shape of the γERSP response at sites with a face-N200 (N = 17) was essentially identical to response at sites without a face-N200 (N = 22). The only notable difference was a reduction in the magnitude of the gamma response at the latter sites (Supplementary Figure 3), consistent with the positive correlation reported above.

We next calculated the grand-average ERP from the 22 electrodes that showed a face-γERSP without a concomitant

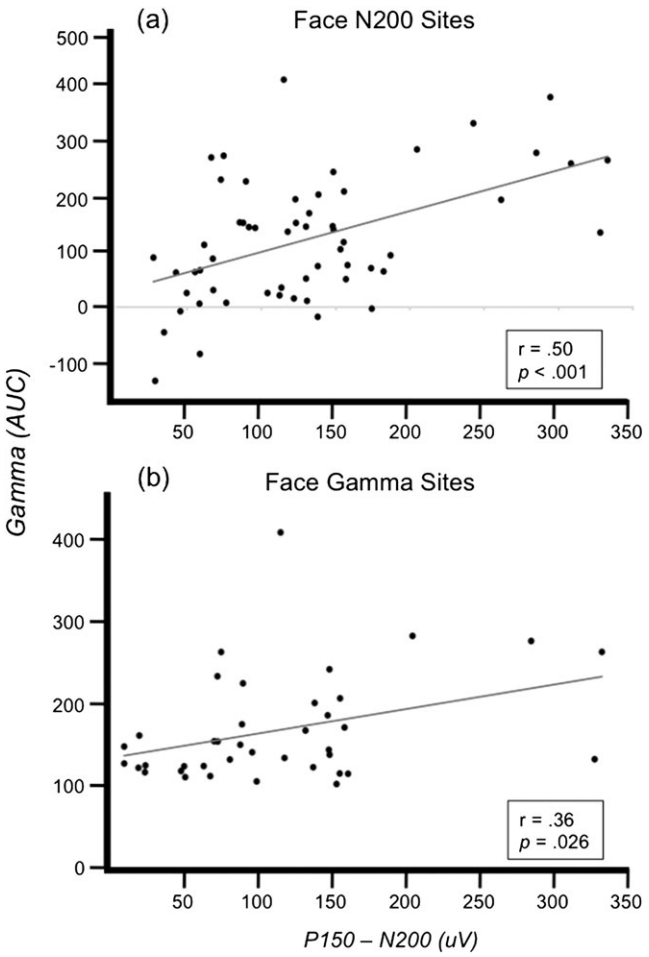

Figure 5. ERP and ERSP relationship. Correlation between gamma amplitude (AUC) and N200 amplitude (measured relative to P150) at (*a*) sites defined by face-N200 and at (*b*) sites defined by face-γERSP.

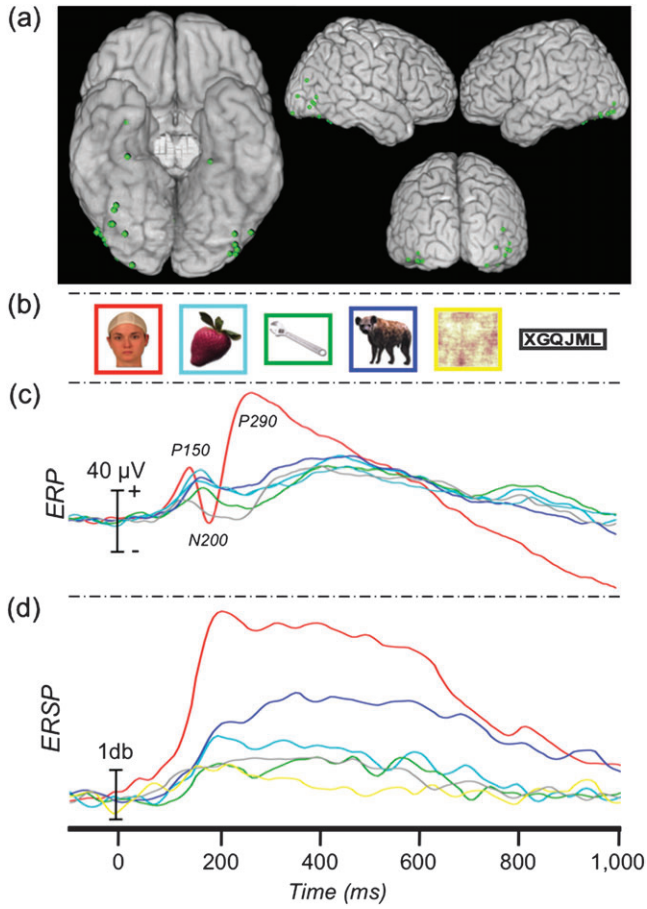

Figure 6. Evoked response at γERSP sites. (*a*) Location of 22 γERSP sites without a concomitant face-N200 (see Materials and Methods). (*b*) Example stimuli presented to patients in Experiment 1. (*c*) The grand-average ERP at these locations. (*d*) The average γERSP time course at these sites.

face-N200 (Fig. 6*c*). Visual inspection of the grand-averaged ERP showed a triphasic waveform characteristic of a face-evoked response composed of a P150, N200, and P290 (Fig. 6*c*, Table 2); all canonical components of a face-specific ERP (cf. Allison et al. 1999). The entire ERP is shifted positively compared with a typical face-ERP resulting in a small amplitude N200 (mean = –2.08 μV) and an exaggerated P290 component. However, neither the N200 nor the P290 was significantly correlated with the AUC of the γERSP, P values > 0.05.

Finally, we investigated the relationship of the ERP and γERSP across all 39 face-γERSP sites. We found a significant positive linear relationship between the magnitude of the γERSP and the amplitude of the face-N200 (measured relative to P150), $r_{(37)} = 0.36$, $P = 0.026$ (Fig. 5b).

Experiment 2—Featural Complexity: ERP

We recorded from 4736 sites from 37 patients in Experiment 2. Sixty-four (1.35%) face-specific sites were identified from 27 patients, primarily along the VOTC and adjacent lateral regions including inferior and middle temporal and inferior occipital and middle occipital cortices (Fig. 7*a*). These 27 patients each had between 1 and 8 (median = 2) face-specific sites. Thirty-three of these face-N200 sites were in common with those identified Experiment 1.

Table 2
Experiment 1: ERP latency and amplitude at face-γERSP sites that do not have a face-N200 ($N = 22$)

Condition	Amplitude (μV)		Latency (ms)	
	Mean	SD	Mean	SD
Faces	−51.6	88.0	187.2	16.2
Fruits	−10.4	51.8	208.2	28.5
Tools	−14.8	41.8	212.4	31.0
Animals	−18.8	62.9	210.1	25.5
Scrambled faces	−7.9	47.3	209.3	29.0
Letter strings	−32.9	57.2	195.8	33.7

Note: SD, standard deviation.

ANOVA showed a significant main effect of stimulus category (complex faces, simple faces, or greeble objects) on the peak amplitude of the evoked response ($F_{2,126} = 23.34$, $P < 0.001$) (Fig. 7*c*, Table 3). Planned comparisons showed that all pairwise differences were significant. The peak response to greebles was smaller than to both complex ($t_{(63)} = 5.94$, $P < 0.001$) and simple ($t_{(63)} = 4.37$, $P < 0.001$) faces. The peak response to complex faces was larger than to simple faces ($t_{(63)} = 2.38$, $P = 0.02$).

Similarly, a separate ANOVA showed a significant main effect of stimulus category on the peak latency ($F_{2,126} = 11.32$, $P < 0.001$) of the evoked response at face-N200 sites. Planned comparisons showed that the peak latency to greebles was

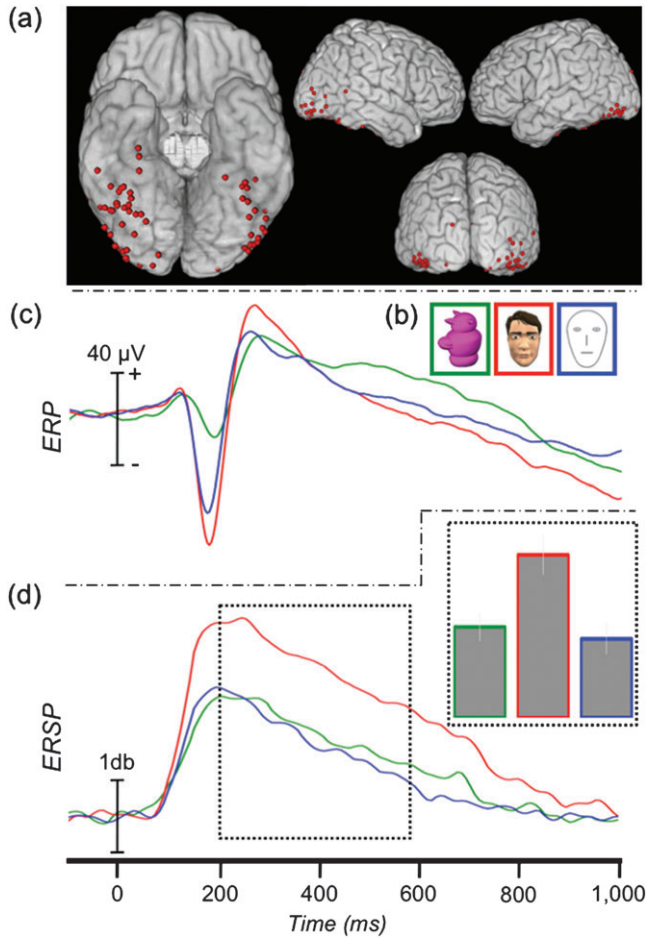

Figure 7. ERP and ERSP to featurally complex and simple faces. (*a*) Location of 64 face-N200 sites displayed on a standard brain. (*b*) Example stimuli presented to patients in Experiment 2. (*c*) The grand-average ERP at the face-N200 sites. (*d*) The average γERSP time course at the face-N200 sites and AUC (inset).

significantly later than to both complex ($t_{(63)}$ = 3.35, P = 0.001) and simple ($t_{(63)}$ = 3.57, P < 0.001) faces. There was no significant latency difference between complex and simple faces ($t_{(63)}$ = 1.00, P = 0.321).

Experiment 2—Featural Complexity: γERSP

ANOVA showed a significant main effect of stimulus category on gamma amplitude ($F_{2,126}$ = 26.86, P < 0.001) (Fig. 7*d*, Table 3). Planned comparisons showed that the complex faces induced a significantly larger γERSP than both simple faces ($t_{(63)}$ = 8.06, P < 0.001) and greebles ($t_{(63)}$ = 4.80, P < 0.001). There was no difference between simple faces and greebles ($t_{(63)}$ = 1.06, P = 0.293).

Discussion

We have shown that face-induced gamma oscillations and face-specific ERPs can be functionally dissociated even when recorded from the same electrode sites. These different response properties suggest that different stages of face processing can occur in the same cortical loci and that the hierarchy of face processes identified in psychological models (e.g., Bruce and Young 1986) is not exclusively reflected in progression through separate cortical regions. Prior to a full discussion of these functional dissociations, we first review the spatial relationship of face-γERSPs and face-N200s.

Table 3
Experiment 2: ERP and ERSP (AUC between 200 and 600 ms) response at face-N200 sites (N = 64)

Condition	ERP				ERSP	
	Amplitude (μV)		Latency (ms)		Gamma AUC (db^2)	
	Mean	SD	Mean	SD	Mean	SD
Greeble objects	−25.7	42.3	193.3	25.3	52.2	65.2
Complex faces	−75.4	70.3	183.4	18.6	93.6	91.2
Simple faces	−62.3	57.5	182.3	20.7	45.3	69.5

Note: SD, standard deviation.

Colocalization of Face-γERSP and Face-N200

To date, there has been mixed evidence as to the spatial independence of the face-γERSP and face-N200; that is, whether induced gamma could appear at sites without a concomitant evoked response and vice versa. Lachaux et al. (2005) emphasized the spatial independence of these neural phenomena, reporting some electrode sites with evoked responses and no induced gamma and other sites with induced gamma and no evoked response. However, Fisch et al. (2009) reported that 18 of 20 sites with category-specific gamma also had an early negative evoked component. Similar to the latter finding, we found that 95% (37 of 39) of face-γERSP sites also had a face-evoked N200. Seventeen of these sites were independently identified as having face-specific evoked responses; 20 of the remaining 22 sites did not meet our conservative "specificity" criteria, but, nonetheless, evinced a clear face-evoked potential (Fig. 6*c*) that was larger than the ERP evoked by any other stimulus category. In any case, the presence of face-γERSP almost perfectly predicted the presence of a face-N200. Moreover, the magnitude of the gamma response at face-γERSP sites was positively correlated with the size of the face-N200. Conversely, the presence of a face-N200 did not completely predict the presence of face-induced gamma. Although there was a positive relationship between the magnitude of the face-N200 and γERSP at face-N200 sites, a number of these sites evinced a face-N200 without a notable increase in gamma power. As discussed further below, impoverished face stimuli elicited robust face-N200s but no face-γERSP.

Thus, while face-γERSPs were almost always associated with face-N200s, the converse was not true. This could be due to high-frequency oscillations suffering a steeper decline in signal-to-noise as a function of distance from the neural source. This would be consistent with prior results showing greater spatial specificity in the high than low-frequency bands (cf., Jerbi et al. 2009). It is also possible that the phase-locked N200 may only appear to have a larger local spatial distribution by virtue of volume conduction and the improved signal-to-noise of time-locked fields by signal averaging. Indeed, the grand-averaged evoked response from sites immediately adjacent (≤10 mm) to face-N200 locations showed a small, but clearly evident face-evoked potential (Fig. 3*b*) whereas the face-γERSP was completely absent at these same electrode locations (Fig. 3*c*). Alternatively, this difference may reflect as yet unknown differences in the functional specialization of the underlying neural responses as discussed further below.

Functional Dissociations between Face-γERSP and Face-N200

When restricting our analysis to face-N200 sites identified by criteria described in the Materials and Methods, we found that γERSP and N200 were differentially modulated by both between-category (face and animal) and within-category (simple vs. complex faces) stimuli. At face-N200 sites, the N200 evoked by animals was larger than to all other nonface categories. This is consistent with previous research showing that frontal images of the faces of cats and dogs evoke face-N200s that are approximately 75% as large as those evoked by human faces (McCarthy et al. 1999). Similarly, the γERSP induced by images of animals at these sites was also larger than to all other nonface categories. However, in the current experiment, the animal stimulus set was composed of images that varied with regard to the orientation and visibility of the face, affording us the opportunity to analyze separately those images with and without a clearly visible face. Unsurprisingly, the N200 and γERSP were largest in response to images of human faces and animals with a highly visible face. Importantly, however, the γERSP induced by animal images without a highly visible face was significantly larger than to fruits, whereas there was no such difference in the (very small) N200 evoked by fruits and animals without visible faces. This result suggests that the N200 is dependent on the presence of canonical facial features (e.g., eyes and nose) while the induced γERSP response may also reflect additional processing related, perhaps, to the perception of animal forms.

That the γERSP might support more elaborative processing than structural encoding was further explored in Experiment 2, which compared the N200 and the γERSP responses to simple faces, complex faces, and greebles. As expected, the simple and complex faces each evoked a significantly larger N200 than the greebles. The N200 evoked by complex faces was also somewhat larger than that evoked by simple faces. In strong contrast to the ERP results, however, the γERSP induced by simple faces did not differ from the greeble stimuli, and both were significantly smaller than the γERSP induced by complex faces. This result supports earlier conclusions about N200 as reflecting an obligatory response to the perception of a face (perhaps reflecting structural encoding). However, unlike N200, the γERSP was not induced by the simple face outlines, suggesting that that the induced gamma is not an obligatory response to simple face features, but reflects more elaborative processing. Consistent with this interpretation, Tsuchiya et al. (2008) successfully discriminated between happy and fearful facial expressions by employing a novel time-frequency decoding method based on power modulations between 60 and 150 Hz along the fusiform gyrus. However, they were unable to compare this discrimination performance to the evoked response because their stimuli morphed from neutral to dynamic over 500 ms and therefore lacked a discrete onset time for the emotional face, resulting in the absence of an N200. Importantly, while our data provide strong evidence for functional dissociation of face processing within the same discrete cortical loci of the VOTC, it does not preclude the possibility that the gamma responses reflect coherent neural activity in a network of face processing regions. Similarly, it is possible that it is the gamma response that reflects local processing, whereas the evoked N200 reflects a face-network wide phase resetting of low-frequency oscillations serving to synchronize nodes of the network for subsequent processing and information sharing.

Face-Specific Electrophysiological Responses

The initial reports of face-induced gamma oscillations (Lachaux et al. 2005) were based upon contrasts between visually ambiguous face stimuli (so-called Mooney faces). It was therefore unclear whether the response reflected a face-specific increase in gamma or was related to feature integration of a coherent stimulus (i.e., the face) as the latter is thought to be a hallmark of gamma activity (Singer and Gray 1995; Tallon-Baudry and Bertrand 1999). More recently, Fisch et al. (2009) reported face-induced gamma activity (30–70 Hz) that was larger for faces when compared with houses and man-made objects. The present study generalize these findings further by showing that the face-γERSP specificity holds when compared with a broader set of control categories, including nonhuman biological entities (i.e., animals, fruits and vegetables), and occurs over a wider range of frequencies (30–100 Hz).

Although the current report focuses on the category-specific response to faces, we also observed 22 sites with an N200 specific to our nonword letter-string category, consistent with previous reports of word and nonword category-specific evoked potentials (Allison, McCarthy, et al. 1994; Nobre et al. 1994). A small subset of these sites evinced a letter-string–specific γERSP. Further experiments will be necessary that compare word and nonword letter strings to determine if elaborative processing of words compared with nonwords results in a dissociation of the γERSP similar to what we have reported for complex versus simple faces.

In summary, we report novel characteristics of the face-induced gamma response, and the functional and spatial relationship of the face-induced and face-evoked responses. The γERSP is a category-specific phenomenon that displayed a complex pattern of association and dissociation with the face-N200. The presence of the face-γERSP predicted the presence of the face-N200 at the same electrode site. At such sites, there was a strong positive relationship between the magnitude of the induced gamma and evoked responses. Conversely, the presence of the face-N200 was not sufficient to predict the presence of the face-γERSP. Indeed, impoverished minimal face line drawings evoked a robust face-N200 but did not induce a category-specific face-γERSP. Taken together, these results suggest that the face-induced gamma response reflects elaborative processing of faces, while face-N200 may reflect a synchronizing event within the face network that may, or may not, result in such elaborative processing.

Supplementary Material

Supplementary Figures 1–3 can be found at: http://www.cercor.oxfordjournals.org/.

Funding

National Institutes of Health (grants MH05286 and NS41328).

Notes

We thank Drs Truett Allison, Kenneth A. Vives, and Dennis D. Spencer and Mr Joseph Jasiorkowski for their help in acquiring the intracranial EEG data reported here. We also thank Mr William Walker for assistance in data collection and electrode localization. *Conflict of Interest*: None declared.

References

Allison T, Ginter H, McCarthy G, Nobre AC, Puce A, Luby M, Spencer DD. 1994. Face recognition in human extrastriate cortex. J Neurophysiol. 71:821–825.

Allison T, McCarthy G, Nobre A, Puce A, Belger A. 1994. Human extrastriate visual cortex and the perception of faces, words, numbers, and colors. Cereb Cortex. 4:544.

Allison T, Puce A, Spencer DD, McCarthy G. 1999. Electrophysiological studies of human face perception. I: potentials generated in occipitotemporal cortex by face and non-face stimuli. Cereb Cortex. 9:415–430.

Baylis GC, Rolls ET, Leonard CM. 1985. Selectivity between faces in the responses of a population of neurons in the cortex in the superior temporal sulcus of the monkey. Brain Res. 342:91–102.

Bruce C, Desimone R, Gross CG. 1981. Visual properties of neurons in a polysensory area in superior temporal sulcus of the macaque. J Neurophysiol. 46:369–384.

Bruce V, Young A. 1986. Understanding face recognition. Br J Psychol. 77:305–327.

Delorme A, Makeig S. 2004. EEGLAB: an open source toolbox for analysis of single-trial EEG dynamics including independent component analysis. J Neurosci Methods. 134:9–21.

Engell AD, McCarthy G. 2010. Selective attention modulates face-specific induced gamma oscillations recorded from ventral occipitotemporal cortex. J Neurosci. 30:8780–8786.

Fisch L, Privman E, Ramot M, Harel M, Nir Y, Kipervasser S, Andelman F, Neufeld MY, Kramer U, Fried I, et al. 2009. Neural "ignition": enhanced activation linked to perceptual awareness in human ventral stream visual cortex. Neuron. 64:562–574.

Gauthier I, Tarr MJ. 1997. Becoming a "Greeble" expert: exploring mechanisms for face recognition. Vision Res. 37:1673–1682.

Gross CG, Rocha-Miranda CE, Bender DB. 1972. Visual properties of neurons in inferotemporal cortex of the macaque. J Neurophysiol. 35:96–111.

Haxby JV, Horwitz B, Ungerleider LG, Maisog JM, Pietrini P, Grady CL. 1994. The functional organization of human extrastriate cortex: a PET-rCBF study of selective attention to faces and locations. J Neurosci. 14:6336–6353.

Jerbi J, Ossandón T, Jung J, Minotti M, Bertrand B, Berthoz B, Kahane P, Lachaux JP. 2009. Task-related gamma-band dynamics from an intracerebral perspective: review and implications for surface EEG and MEG. Hum Brain Mapp. 30:1758–1771.

Kanwisher N, McDermott J, Chun MM. 1997. The fusiform face area: a module in human extrastriate cortex specialized for face perception. J Neurosci. 17:4302–4311.

Kiani R, Esteky H, Mirpour K, Tanaka K. 2007. Object category structure in response patterns of neuronal population in monkey inferior temporal cortex. J Neurophysiol. 97:4296.

Lachaux JP, George N, Tallon-Baudry C, Martinerie J, Hugueville L, Minotti L, Kahane P, Renault B. 2005. The many faces of the gamma band response to complex visual stimuli. Neuroimage. 25:491–501.

Leonard CM, Rolls ET, Wilson FAW, Baylis GC. 1985. Neurons in the amygdala of the monkey with responses selective for faces. Behav Brain Res. 15:159–176.

McCarthy G. 2001. Physiological studies of face processing in humans. In: Gazzaniga MS, editor. The new cognitive neurosciences. Cambridge (MA): MIT Press. p. 393–409.

McCarthy G, Puce A, Belger A, Allison T. 1999. Electrophysiological studies of human face perception. II: response properties of face-specific potentials generated in occipitotemporal cortex. Cereb Cortex. 9:431–444.

Nobre AC, Allison T, McCarthy G. 1994. Word recognition in the human inferior temporal lobe. Nature. 372:260–263.

Perrett DI, Rolls ET, Caan W. 1982. Visual neurones responsive to faces in the monkey temporal cortex. Exp Brain Res. 47:329–342.

Pinsk MA, DeSimone K, Moore T, Gross CG, Kastner S. 2005. Representations of faces and body parts in macaque temporal cortex: a functional MRI study. Proc Natl Acad Sci U S A. 102:6996–7001.

Puce A, Allison T, Gore JC, McCarthy G. 1995. Face-sensitive regions in human extrastriate cortex studied by functional MRI. J Neurophysiol. 74:1192–1199.

Puce A, Allison T, McCarthy G. 1999. Electrophysiological studies of human face perception. III: effects of top-down processing on face-specific potentials. Cereb Cortex. 9:445–458.

Puce A, Allison T, Spencer SS, Spencer DD, McCarthy G. 1997. Comparison of cortical activation evoked by faces measured by intracranial field potentials and functional MRI: two case studies. Hum Brain Mapp. 5:298–305.

Sergent J, Ohta S, MacDonald B. 1992. Functional neuroanatomy of face and object processing: a positron emission tomography study. Brain. 115:15.

Singer W, Gray CM. 1995. Visual feature integration and the temporal correlation hypothesis. Annu Rev Neurosci. 18:555–586.

Spencer SS, Spencer DD, Williamson PD, Mattson RH. 1982. The localizing value of depth electroencephalography in 32 patients with refractory epilepsy. Ann Neurol. 12:248–263.

Tallon-Baudry C, Bertrand O. 1999. Oscillatory gamma activity in humans and its role in object representation. Trends Cogn Sci. 3:151–162.

Tsao DY, Freiwald WA, Knutsen TA, Mandeville JB, Tootell RB. 2003. Faces and objects in macaque cerebral cortex. Nat Neurosci. 6:989–995.

Tsuchiya N, Kawasaki H, Oya H, Howard MA, Adolphs R. 2008. Decoding face information in time, frequency and space from direct intracranial recordings of the human brain. PLoS One. 3:3892.